Wind Farm Layout Optimization on Complex Terrains – Integrating a CFD Wake Model with Mixed-Integer Programming

Jim Y. J. Kuo[1], David A. Romero, J. Christopher Beck, Cristina H. Amon

Mechanical and Industrial Engineering, University of Toronto, Toronto, Ontario, Canada

Abstract

In recent years, wind farm optimization has received much attention in the literature. The aim of wind farm design is to maximize energy production while minimizing costs. The wind farm layout optimization (WFLO) problem on uniform terrains has been tackled by a number of approaches; however, optimizing wind farm layouts on complex terrains is challenging due to the lack of accurate, computationally tractable wake models to evaluate wind farm layouts. This paper proposes an algorithm that couples computational fluid dynamics (CFD) with mixed-integer programming (MIP) to optimize layouts on complex terrains. CFD simulations are used to iteratively improve the accuracy of wake deficit predictions while MIP is used for the optimization process. The ability of MIP solvers to find optimal solutions is critical for capturing the effects of improved wake deficit predictions on the quality of wind farm layout solutions. The proposed algorithm was applied on a wind farm domain in Carleton-sur-Mer, Quebec, Canada. Results show that the proposed algorithm is capable of producing excellent layouts in complex terrains.

Keywords: Wind Farm, Layout Optimization, Complex Terrains, Micro-siting

[1]Corresponding author: jyjkuo@mie.utoronto.ca

1. Introduction

The main objective of a wind farm is to maximize energy production while minimizing costs. The power production of a wind farm is dependent on the incoming wind speeds, which are themselves dependent on terrain topography, atmospheric conditions, and upstream turbine wakes. In particular, production loss due to the wake interference of upstream turbines, called *wake losses* (Fig. 1), can reduce the annual energy of a wind farm by as much as 10% to 20% [1]. In the wind farm layout optimization (WFLO) problem, therefore, minimizing wake losses is crucial.

Most studies have focused on optimizing layouts on flat and uniform topography [2, 3, 4, 5, 6, 7]. However, wind speeds over complex terrains are very different than they are over flat terrains, since complex flow structures can form as wind flows over various land features. Consequently, turbine power production is strongly influenced by local topography. Furthermore, the lack of analytical, closed-form mathematical models for wakes over complex terrains makes it difficult to evaluate and optimize wind farm layouts. As a result, Feng and Shen [8] modified an adapted Jensen wake model to estimate the wake effects of a wind farm on a two-dimensional Gaussian hill. Taking a different approach, the virtual particle model developed by Song et al. [9] modeled the turbine wake as concentration of non-reactive particles undergoing a convection-diffusion process in a relatively low-cost model that describes the wake more accurately than a modified flat terrain wake model. Despite these efforts, reducing the computational cost of wake evaluations while maintaining accuracy during the optimization process remains a challenge. Hence, subsequent work [10, 11, 12] has focused on better integration of wake modeling and optimization algorithms.

Computational fluid dynamics (CFD) models (e.g. actuator disk and actuator line) have been developed to simulate complex wake phenomena and their interactions with terrains [13, 14, 15, 16, 17, 18, 19]. However, these simulations are expensive and must be used sparingly during the optimization process.

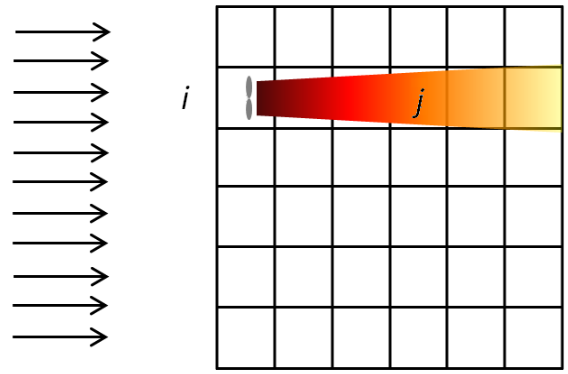

Figure 1: Turbine wake created by west wind. The wake from turbine at location i propagates downstream, affecting location j.

Deterministic optimization approaches such as mixed-integer programming (MIP) [2, 3, 20, 21, 22] have been shown to be promising in solving WFLO problems. These models can provide global solutions and optimality bounds for relatively small problems. In a MIP model, the wind farm is divided into discrete number of turbine locations and the wake interactions are calculated in advance for algorithms such as branch and bound [3, 20, 23, 24, 25], to be applied to solve the WFLO problem.

The objective of this paper is to introduce an algorithm capable of integrating CFD simulation data to intelligently optimize wind farm layouts located on complex terrains. In the proposed algorithm, CFD simulations are used as input for MIP to improve the accuracy of the wake effects. Conversely, MIP provides information on the promising turbine locations where CFD simulations should be conducted. This two-way coupling between MIP and CFD reduces the number of CFD simulations significantly, and in turn the computational cost. This algorithm is applied on a terrain found in Carleton-sur-Mer, Quebec, Canada. Results show that the algorithm is capable of optimizing layouts of wind farms on complex terrains by integrating CFD simulation data into the optimization process.

2. Previous Work

2.1. Optimization Models

A number of approaches to tackle the WFLO have been developed in the literature. The WFLO problem can be modeled by two approaches, discrete and continuous. In discrete models [4, 5, 26], the wind farm domain is divided into a number of possible turbine locations, while for continuous models [27, 28, 29, 30, 31, 32, 33], the turbine location is represented by two-dimensional continuous coordinates. Continuous models are typically solved using evolutionary metaheuristic algorithms [31, 34, 35, 36, 37, 32, 38, 39, 40] and nonlinear optimization methods [41, 42]. A discrete model can be solved by using mathematical programming approaches, which have the significant advantage of providing optimality bounds [3, 20, 24, 25, 6].

2.2. CFD Models

Computational fluid dynamics models have been applied to simulate wind turbine wakes, using Reynolds-averaged Navier-Stokes (RANS) [13, 14] and Large Eddy Simulation (LES) [15, 43, 44, 45, 46] turbulence models to simulate the turbulent wake phenomena. In addition to turbulence modeling, there are two main approaches to model rotor geometry: actuator disk/line and direct blade modeling. In an actuator disk [13, 14, 16, 47, 48, 49] or actuator line [50, 51, 52] approach, the turbine is modeled by imposing aerodynamic forces through a disk representing the rotor or lines representing the turbine blades, respectively. In a direct blade modeling approach [44, 53, 54], the turbine geometries are inserted into the computational domain, allowing a more accurate representation of the aerodynamic effects than the actuator disk/line approach at the expense of higher computational cost. The actuator disk approach is less computationally expensive and less accurate. Despite the introduction of these models in turbine wake modeling, it remains difficult to apply these models in optimization algorithms to solve the WFLO problem due to the computational expense of CFD models.

3. Proposed WFLO Optimization Algorithm

While optimization and wake modeling have been applied individually to WFLO, there is a significant challenge in combining them. An optimization algorithm typically must evaluate a very large number of solutions and partial solutions. However, a single CFD simulation is so computationally expensive that very few can be conducted in a reasonable run-time. In our approach, the optimization model is first used with less accurate, less expensive data to identify promising turbine locations. The wake effects of turbines placed at those locations are updated using CFD simulations. The CFD data is then used iteratively by the optimization model to identify newly promising locations. Figure 2 shows a schematic of our approach.

The principal idea behind the proposed algorithm is that on a complex terrain, the wind energy potential of a location is influenced by the local terrain topography, thus different turbine locations will have different "turbine placement potentials". The proposed algorithm utilizes a MIP model to search through promising locations through a combination of estimated wake effects and CFD simulation data.

Looking at the flowchart of the proposed algorithm in Fig. 2, firstly, a flow field over the complex terrain without turbines is generated using CFD. The initial wake effects can be calculated by superimposing a flat terrain wake onto the complex terrain as described in Section 3.2. This initial problem is then solved to determine where the turbines should be placed. However, due to inaccuracies in the initial wake estimate, placing turbines at these locations may not produce the optimal layout. Hence CFD simulations are conducted at these locations to improve the accuracy of the initial estimated wake effects. This process is repeated until no new improving turbines locations are found. In other words, the wake effects described in the optimization model becomes more accurate with each iteration. Hence, the optimal solution of the current iteration is more accurate than those found in previous iterations. If the problem cannot be solved to optimality due to run-time limits, then it becomes necessary

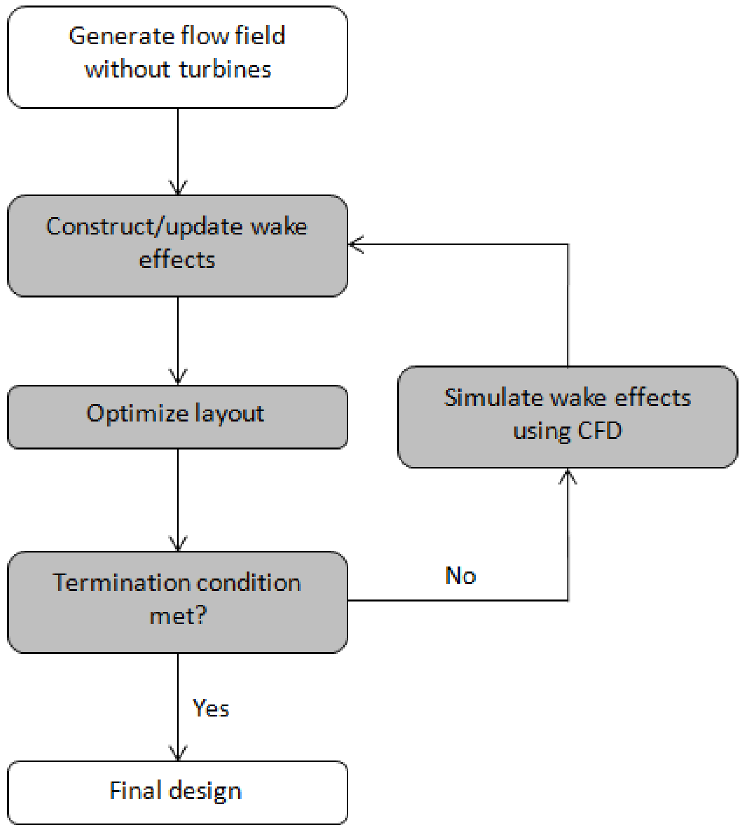

Figure 2: Flowchart of the optimization algorithm process

to compare the near-optimal solutions from previous iterations. Conceivably, other optimization methods such as metaheuristics are also compatible with this algorithm; however, without proof of optimality, the termination criteria for the optimization problem would need to be defined appropriately.

3.1. MIP Optimization Model

A number of mixed-integer programming formulations have been developed to tackle the WFLO problem [3, 20, 21, 22]. A MIP model consists of an objective function, a set of constraints, and a mix of integer and continuous variables. To describe the WFLO problem, the wind farm is discretized into possible turbine locations with corresponding binary decision variables denote if a turbine is located at each location or not. The formulation used in this work, identical to that of the work of Kuo et al. [21, 22], has an objective function of maximizing the sum of the kinetic energy experienced by each turbine, as follows. Let the wind farm domain be divided into a total of N cells, let K be the number of turbines to be placed (considered a constant in the formulation), and let x_i be a binary variable denoting whether a turbine is placed in the i-th cell. The optimization problem is

$$\max \sum_{i=1}^{N} \sum_{s \in S} p_s x_i \Big[U_{0,s,i}^2 - \sum_{j \in J} (U_{0,s,j}^2 - u_{s,ij}^2) x_j \Big] \tag{1a}$$

$$\text{s.t} \quad \sum_{i=1}^{N} x_i = K \tag{1b}$$

$$d_{ij} x_i + d_{ji} x_j \leq 1 \qquad \forall i, j \tag{1c}$$

$$x_i \in \{0, 1\} \qquad \forall i = 1, ..., N \tag{1d}$$

where the binary terms d_{ij} and d_{ji} indicate the violation of the distance constraint between i-th and j-th cells, which need to be calculated in advance. Namely, $d_{ij} = d_{ji} = 1$ if the distance constraint is violated when turbines are placed both in the i-th and j-th locations, and $d_{ij} = d_{ji} = 0$ otherwise. In Eq.(1a), p_s is the probability of wind state s, and S is the total number of wind states, where a wind state is defined as a (wind speed, wind direction) pair. Most importantly, $U_{0,s,j}^2 - u_{s,ij}^2$ denotes the kinetic energy deficit at cell j caused by a turbine at cell i, which is dependent on the wind state, s. Figure 1 shows a wake from turbine located in cell i, propagating downstream to affect cell j.

In this formulation, all the single wake effects caused by a turbine must be calculated in advance for all possible locations. That is, when a turbine is placed in cell i, its single wake effects on all remaining cells must be known for all possible turbine locations and wind states. Hence, the number of potential turbine locations (i.e., the number of cells) multiplied by the number of wind states determines the number of wake calculations required (i.e., $N|S|$) to define the

MIP formulation. In the proposed algorithm, the promising turbine locations are identified from the optimal MIP layout solutions using less accurate data and CFD simulations are only conducted at these locations. In this way, we seek to achieve the same wake accuracy as running $N|S|$ CFD simulations with a fraction of the computational cost.

When multiple turbines wakes are present, their combined effect on wind speed recovery is approximated by using an energy balance approach by Kuo et al. [22]. This form is suitable for MIP formulation due to its linearity and sound physical basis. Energy balance is done along a streamtube from the free stream mixing into the wake, assuming the wake losses are additive for overlapping wakes. The MIP model can be solved using mathematical programming approaches to compute the optimal turbine layout for each set of inputs.

3.2. Wake Modeling

In order to identify a promising turbine placement to evaluate with a CFD simulation, we must first solve the MIP model with approximate wake effects. These wake effects are calculated using an approximate wake model by superimposing CFD simulation data of a flat terrain wake onto the complex terrain, using Eq.(2) and Eq.(3). The assumptions made here are that the wake propagates downstream along the terrain surface at hub height and that the wake will experience a speed-up factor due to terrain effects, i.e.

$$u_{ct,s,j} = S_{s,j} u_{ft,s,j}, \tag{2}$$

$$u^w_{ct,s,ij} = S_{s,j} u^w_{ft,s,ij}, \tag{3}$$

where $u_{ct,s,j}$ and $u_{ft,s,j}$ are the free stream wind speeds on complex and flat terrains in cell j in wind state s, and $u^w_{ct,s,ij}$ and $u^w_{ft,s,ij}$ describe the wind speeds in the wake on complex and flat terrains in cell j due to a turbine in cell i, respectively. In other words, $S_{s,j}$, the speed-up factor due to terrain effects experienced in cell j (in comparison with flat terrain flow field) in wind state s, is calculated without the presence of turbines, and then used to "carry" the wakes downstream, similar to the implementation used by Feng and Shen [8] and in several commercial software packages [8]. In this work, whenever CFD simulation data is available, the speed-up factor $S_{s,j}$ is corrected using simulation results. It should be noted that while superimposing wakes onto terrains is not an accurate representation of the actual wake effects, this work also addresses the effects of accuracy of initial wake approximation on solution quality and computational cost (see following section).

When promising turbine locations are available, CFD simulations are conducted to simulate wake effects of turbines at those locations. The actuator disk model and the extended $k - \epsilon$ turbulence model by El Kasmi and Masson [55] are used in this study. Specifically, an actuator disk is inserted into the computational domain and the turbulent dissipation zones are prescribed upstream and downstream of the disk, shown in Fig. 3. Appropriate boundary conditions (e.g. inlet, outlet, surface roughness) must be prescribed to accurately simulate the atmospheric boundary layer.

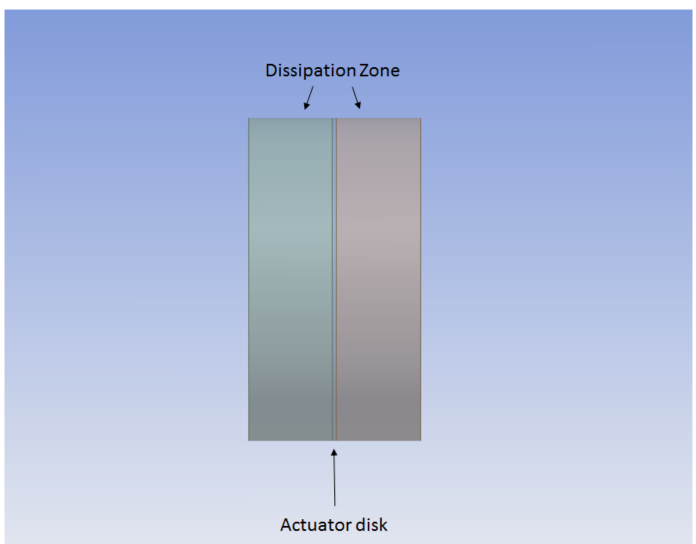

Figure 3: Actuator disk model by El Kasmi and Masson [55].

To summarize how MIP and CFD are combined, the proposed algorithm is as follows:

(1) Generate flow field over the complex terrain without turbines using CFD.

(2) Construct the initial wake effects using the approximated method described in wake modelling section.

(3) Solve the optimization problem to identify the most promising locations.

(4) Run single turbine CFD simulations at locations found in the previous step.

(5) Update the wake effects from CFD results ($u_{s,ij}$ term) in optimization (Eq.(1a)).

(6) Repeat steps (3–5) until the solution converges.

3.3. Impact of the Initial Wake Approximation

In this algorithm, the final layout is dependent on the initial wake approximation. The assumption that wakes propagate in a straight line at the hub height may not hold for complex terrains, thus resulting in a vast overestimate of the velocity deficit in certain cells and an underestimate in others. If the velocity deficit is overestimated in some cells in the initial approximation, those cells might never be considered in future layout solutions. Thus a relaxation parameter, C, is introduced to reduce the velocity deficit in the initial wake approximation. Specifically, the velocity deficit is multiplied by the relaxation parameter, C, to force an underestimate of the velocity deficit and mitigate the effect of poor approximations of wake behavior on complex terrains.

When the wake effects are underestimated, more turbine locations or cells will be explored so more CFD simulations are required. Hence, the relaxation parameter C controls how aggressively the optimization space is explored, balancing the need for better accuracy in wake modeling with the total computational cost of the optimization. Specifically, the $u_{s,ij}$ term from Eq.(1a) is re-written as $U_{0,s,j} - CD_{s,ij}$, where $D_{s,ij}$ is the velocity deficit at cell j caused by turbine at cell i in wind state s. The $U_{0,s,j} - CD_{s,ij}$ term is only used when CFD data is not available (these cells are defined as set N_2). If CFD data is available (defined as set N_1), then the simulation data is used directly for $u_{s,ij}$

and the relaxation parameter is not used. The new MIP formulation is written as,

$$\max \sum_{i\in N_1}\sum_{s\in S} p_s x_i \Big[U_{0,s,i}^2 - \sum_{j\in J}(U_{0,s,j}^2 - u_{s,ij}^2)x_j\Big] \tag{4a}$$

$$+ \sum_{i\in N_2}\sum_{s\in S} p_s x_i \Big[U_{0,s,i}^2 - \sum_{j\in J}(2U_{0,s,j} - CD_{s,ij})CD_{s,ij}x_j\Big] \tag{4b}$$

$$\text{s.t} \quad \sum_{i=1}^{N} x_i = K \tag{4c}$$

$$d_{ij}x_i + d_{ji}x_j \le 1 \qquad \forall i,j \tag{4d}$$

$$x_i \in \{0,1\} \qquad \forall i = 1,...,N. \tag{4e}$$

4. Case Study: The Carleton-sur-Mer Wind Farm

The proposed algorithm is tested on a 2.8 km x 2.8 km wind farm domain in Carleton-sur-Mer, Quebec, Canada. The topography was extracted from Google Maps$^{\mathrm{TM}}$ (https://goo.gl/maps/XTpxd), with a roughness length assumed to be 0.1 m. The terrain elevation in meters above sea level is shown in Fig. 4. The optimization domain is discretized into a uniform grid of 20 x 20 cells, separated at cell center by a distance of 140 m. A wind farm layout of 20 turbines is optimized for this terrain. The specifications of the turbines are selected to be similar to those in the Carleton Wind Farm, namely, a constant thrust coefficient of 0.8, hub height of 77 m, a rotor diameter of 80 m, and a rated power 1.5 MW. [56]. The proximity constraint between turbines is set as 5 turbine diameters apart.

For this wind farm domain, information regarding the wind speed and directions are available from the Canadian Wind Energy Atlas [57]. A power law velocity profile is used to describe the wind speed at varying heights

$$u(y) = 6\Big(\frac{y-139}{50}\Big)^{0.16}, \tag{5}$$

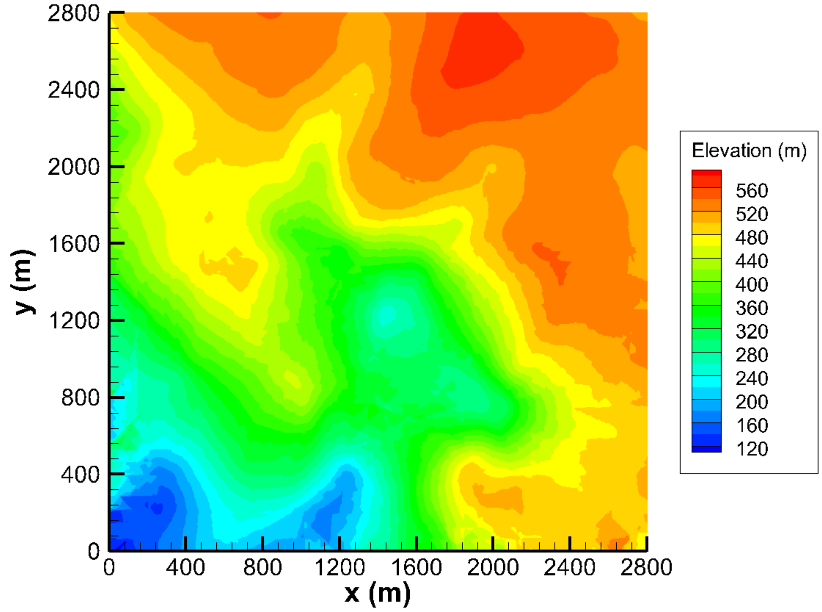

Figure 4: 2.8 km x 2.8 km wind farm domain in Carleton-sur-Mer

where y is the height above sea level. This velocity profile is used to define inlet boundary conditions for CFD simulations. The wind rose used for this domain is shown in Fig. 5, noting that the dominant wind direction is from the west. The turbulent kinetic energy and dissipation rate at the inlet are prescribed as $k = \frac{(u^*)^2}{C_\mu}$ and $\varepsilon(y) = \frac{(u^*)^3}{\kappa(y-139)}$, where $C_\mu = 0.033$ and $\kappa = 0.4$. With the assumptions for ground roughness and the height (1000 m) of the boundary layer, the friction velocity $u^* = 0.4m/s$. The velocity and turbulence quantities are fixed at the top boundary, as other types of boundary conditions such as symmetry or slip wall could cause undesirable streamwise gradients [16, 58]. In case the wind is not aligned with the x-direction, the velocity inlet takes the form of $u_x(y) = 6\left(\frac{y-139}{50}\right)^{0.16} cos(\theta)$ and $u_z(y) = 6\left(\frac{y-139}{50}\right)^{0.16} sin(\theta)$, where θ is the wind direction relative to the x-axis [59]. The ground is taken as wall boundary and the outlet face is considered as pressured outlet boundary.

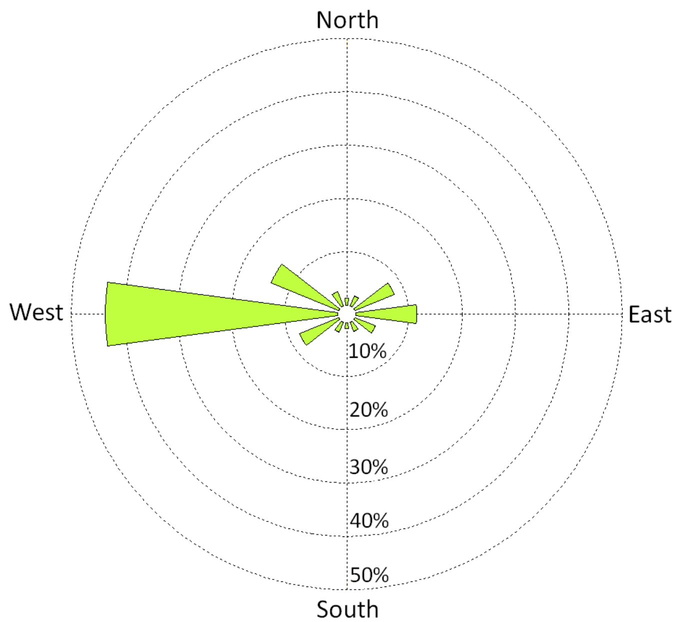

Figure 5: Wind rose for Carleton-sur-Mer. [57]

4.1. Initial Results

To summarize the WFLO problem, 20 turbines are placed in a domain (Fig. 4) that is discretized into uniformly sized 20 x 20 cells. Based on the wind rose, Fig. 5, there are 12 wind directions with a power law wind velocity profile as given in Eq.(5). The proximity constraint between turbines was set to be 5 diameters distance apart. In the initial test, the relaxation parameter has been set to $C = 1$.

The MIP model can be solved under 30 seconds using Gurobi 5.6, so that the bulk of the computational expense is dedicated to CFD simulations. For each cell, a CFD simulation needs to be conducted for every wind direction, or in this case, 12 CFD simulations per cell. With 400 possible locations, and 12 wind directions, the maximum number of single turbine CFD simulations is 400 x 12 = 4800.

Each CFD simulation is performed for a domain of 2.8 km x 2.8 km in length and width, with a height up to 1000 m above sea level, shown in Fig. 6a.

Initially, the CFD simulations are conducted without the presence of turbines for all 12 wind directions, with the domain discretized into 1.2 million cells in the domain. When a turbine is placed in the domain, the number of cells is increased to 1.6 million cells to better capture the wake effects downstream of the turbine, shown in Fig. 6b.

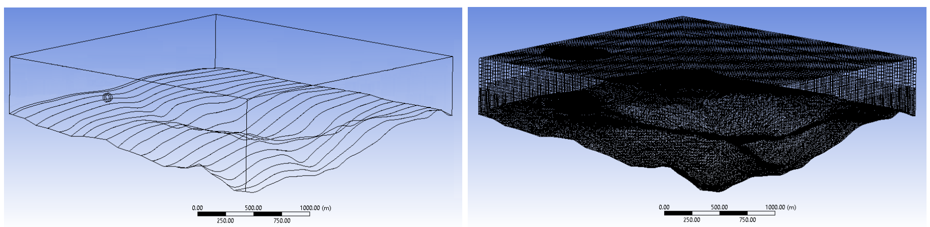

(a) CFD domain with one turbine

(b) Mesh of the CFD domain.

Figure 6: Wind farm domain for CFD simulations

In the first iteration, the flow field in the absence of turbines is obtained from CFD simulations. The turbine wake from flat terrain is modified using Eq.(3) to approximate the wake effects without conducting any CFD wake simulations. The layout found in this first iteration is shown in Fig. 7a.

In the second iteration, the wakes for wind turbines placed at these 20 locations are simulated using CFD and the initial wake effects are updated. The new layout that was found is shown in Fig. 7b. In this new layout, three turbines are relocated compared to the first iteration. The turbine wakes from these three locations (indicated by circles) are simulated and updated. In the third and final iteration, the layout found in Fig. 7c is identical to that of the second layout, indicating that the algorithm has converged.

Note that in the final layout, some turbines are aligned in the prevailing wind direction (west). However, it is important to keep in mind that there are two main factors in optimizing wind farm layouts on complex terrains, wake effects and wind energy potential. As wind speeds are not uniform over a complex terrain domain, it is possible to find a layout in which the algorithm prefers to place a turbine at a location with high energy potential such that it offsets the wake losses.

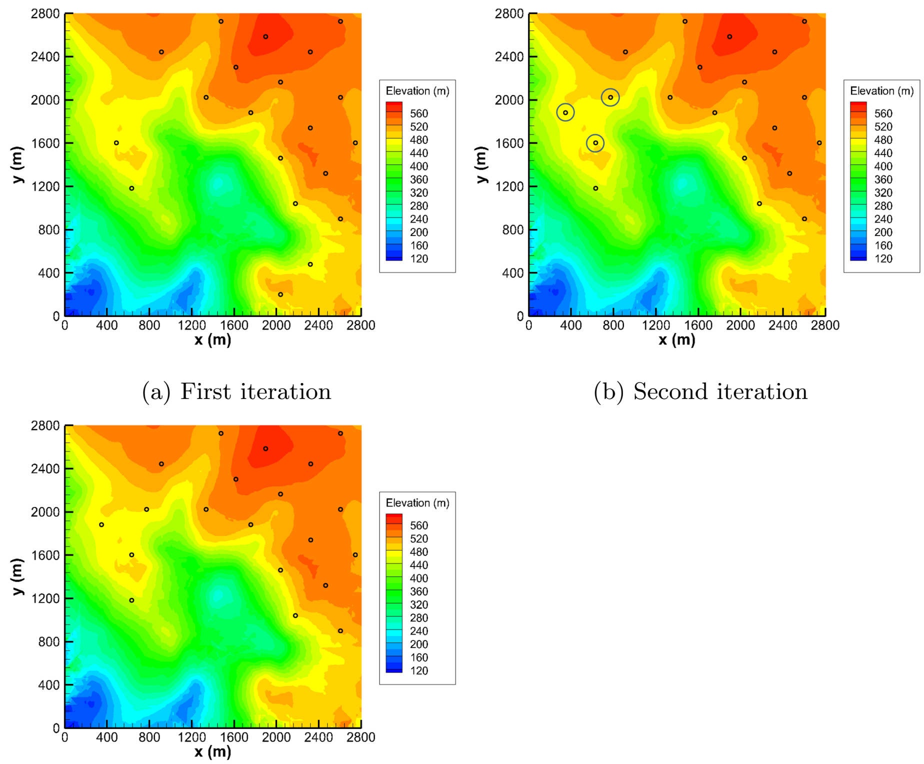

(a) First iteration

(b) Second iteration

(c) Third iteration

Figure 7: Optimal layout found at the end of each iteration. The circles mark the turbines that were relocated in that iteration. Note that after only 3 iterations, the algorithm did not identify additional turbine locations that would lead to improvements in the optimization objective.

4.2. Manipulating the Relaxation Parameter

A parametric study on the relaxation parameter, C, was conducted, considering the values $C = \{1, 0.7, 0.4, 0.2, 0\}$, to study the effects of the initial wake approximation on the solution quality and computational cost. In a WFLO problem for complex terrains, the solution upper bound in terms of energy production is one where the turbines are placed at locations where the wind speeds are the highest, ignoring the wake effects. This upper bound for this test case is found to be 2177.48. Normalizing all the objective values found in this study with this upper bound provides a relative comparison of the solutions found using different values of C. This normalized value is defined as the layout efficiency. The influence of the values of C on the progression on the objective value is shown in Fig. 8.

The solutions found for different values of C are shown in Figs. 9–12. The influence of C on the number of iterations, number of CFD simulations, final objective value, layout efficiency, and run-time is shown in Table 1. It can be seen that as C decreases in value, better layouts are produced. It is notable that for the cases where $C \geq 0.2$, only three iterations and a small fraction of the total number of CFD simulations are needed for convergence. For the case of $C = 0$, eight iterations are required for convergence and more CFD simulations are needed (compared with higher values of C) as the algorithm searched through 52 turbine locations in the domain. In other words, when the wake deficits are not accounted for, the algorithm will "blindly" search through the most promising cells in terms of wind resource until the optimal solution is found. This behavior can be seen in Fig. 12, where large number of turbines are relocated to neighbouring locations from one iteration to the next, until all the promising cells are exhausted. While computational cost is not a major concern when the size of the problem is relatively small, and can be solved to optimality relatively quickly, this can be a significant downside when the problem increases in size, e.g. larger number of possible turbine locations and more complex wind regimes. For the test cases where $C \geq 0.2$, the total run-time is approximately 300 hours on a Dell Precision T1700 PC, but the run-time more than doubled when $C = 0$, demonstrating the importance of the relaxation parameter in controlling the computational cost. It is important to note that the solution found in the $C = 0$ case is the globally optimal solution. That is, if CFD simulation data is available for all cell locations ($N|S| = 4800$ CFD simulations, approximately 5300 hours), the optimal solution would be identical to that of $C = 0$, unless the presence of turbine wakes can locally improve the energy potentials of some locations.

For all the different values of C tested, the final layout solutions are within 2% of the upper bound. The difference in performance between the best ($C = 0$) and worst ($C = 1$) solutions is less than 1.5%, demonstrating the algorithm's capability to find good solutions even with poor initial estimation of wake effects. Figures 13 and 14 show the effects of the relaxation parameter on computational cost and layout efficiency. In terms of solution quality, underestimating the wake deficit (e.g. $C = 0.2$) is desirable as the path of wake propagation is difficult to predict prior to CFD simulations. When higher values of C are used, velocity deficits experienced by downstream turbines may be overestimated in some cells. The consequence is that certain promising locations may be ignored during the search. However, when wake deficits are underestimated with lower values of C, the computational cost increases. In this particular problem, a low C value of 0.2 did not dramatically increase the computational cost relative to larger values, but did improve solution quality significantly. Note that this algorithm is not a globally seeking algorithm, hence the final solution is dependent on the initial layout. Based on the finding, the relaxation factor has the effect of forcing the algorithm to converge into locally optimal solutions.

Choosing the "right" C to produce good layout will depend on the terrain topography. If the terrain is too rugged and the flow experiences rapid changes where the streamlines can deviate significantly from the terrain profile, a smaller C would be ideal in finding good layouts. As the local changes in the topography is less pronounced, a larger value of C would be preferred. An intuitive and adaptive scheme of varying values of C for every iteration can be developed, borrowing the idea from simulated annealing [60], e.g. starting with initial low C and adjusts as the algorithm progresses. In addition, better prediction of the initial wake effect is needed for improving solution quality and computational cost. These two areas of improvement will be the focus in future studies.

Table 1: Influence of relaxation parameter on solution quality and computational cost

C	# of Iterations	# of CFD Evaluations	Final Objective Value	Layout Efficiency (%)	Run-time (hr)
1	3	23 x 12 = 276	2133.25	97.97	303.63
0.7	3	22 x 12 = 264	2146.66	98.58	290.43
0.4	3	21 x 12 = 252	2150.83	98.78	277.23
0.2	3	24 x 12 = 288	2165.16	99.43	316.83
0	8	52 x 12 = 624	2165.80	99.46	686.47

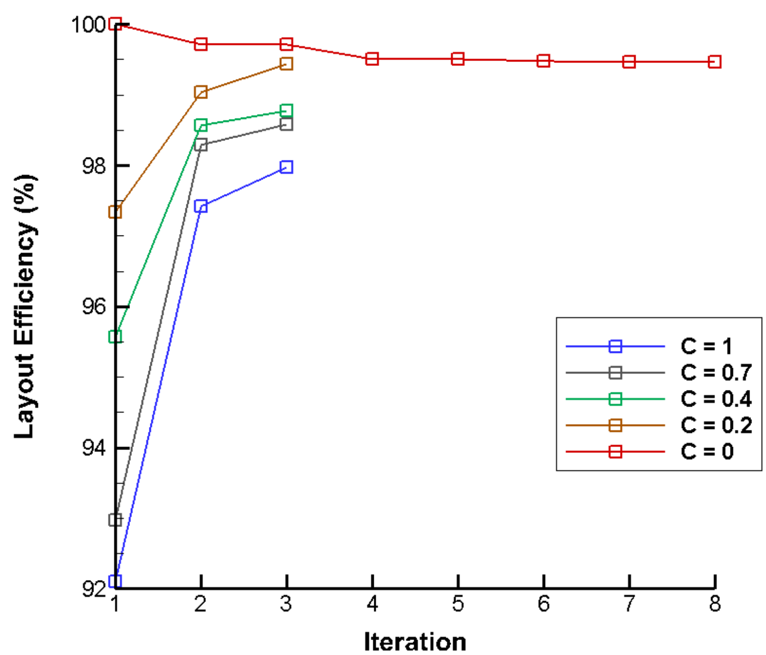

Figure 8: The progression of solutions with varying relaxation values.

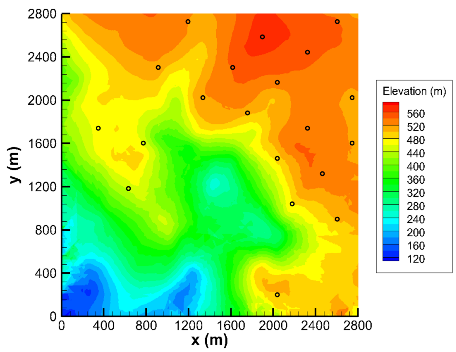

(a) First iteration

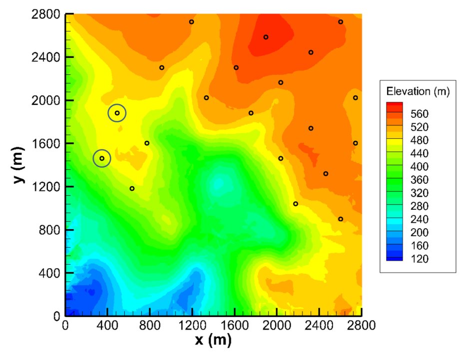

(b) Second iteration

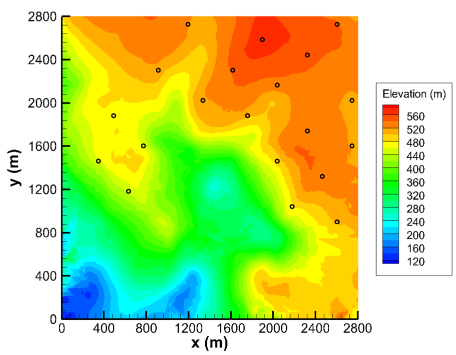

(c) Third iteration

Figure 9: Optimal layout found at the end of each iteration with relaxation parameter, C, set to 0.7. The circles mark the turbines that were relocated in that iteration. Note that after only 3 iterations, the algorithm did not identify additional turbine locations that would lead to improvements in the optimization objective.

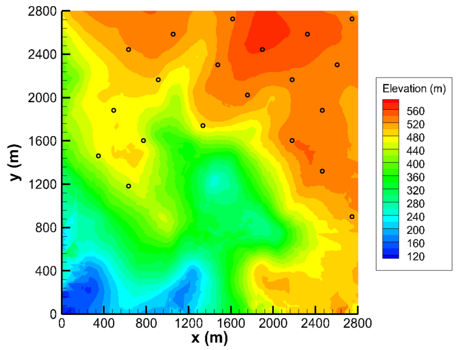

(a) First iteration

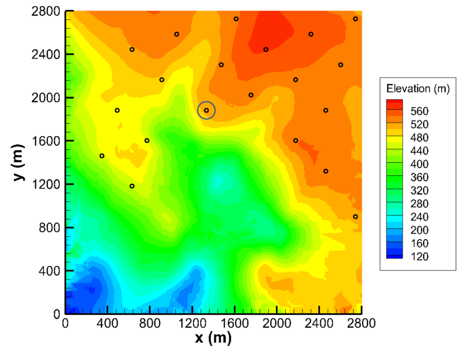

(b) Second iteration

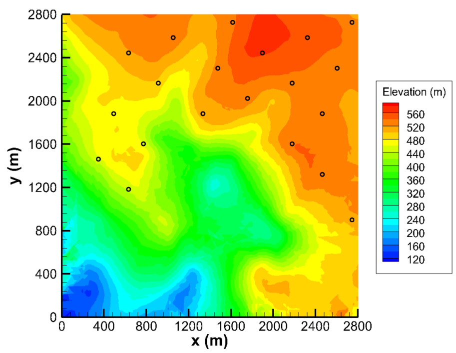

(c) Third iteration

Figure 10: Optimal layout found at the end of each iteration with relaxation parameter, C, set to 0.4. The circles mark the turbines that were relocated in that iteration. Note that after only 3 iterations, the algorithm did not identify additional turbine locations that would lead to improvements in the optimization objective.

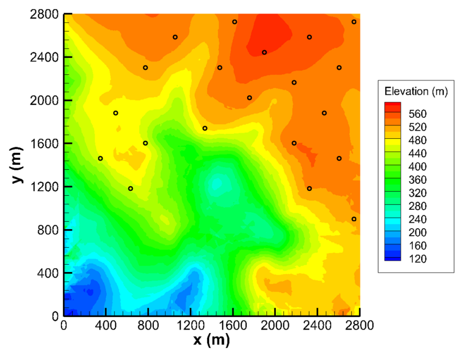

(a) First iteration

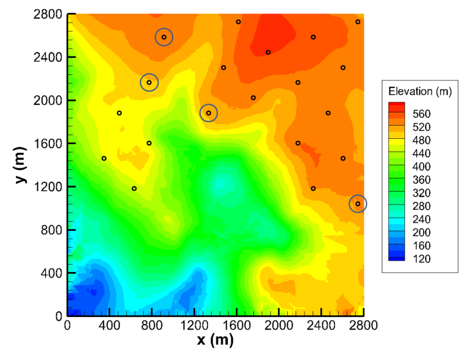

(b) Second iteration

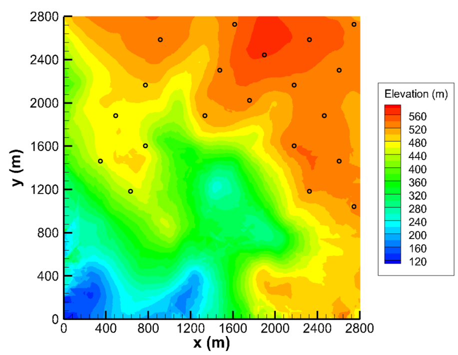

(c) Third iteration

Figure 11: Optimal layout found at the end of each iteration with relaxation parameter, C, set to 0.2. The circles mark the turbines that were relocated in that iteration. Note that after only 3 iterations, the algorithm did not identify additional turbine locations that would lead to improvements in the optimization objective.

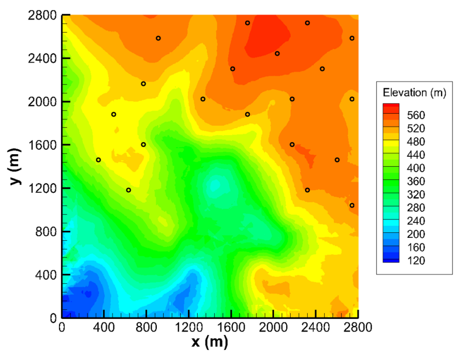

(a) First iteration

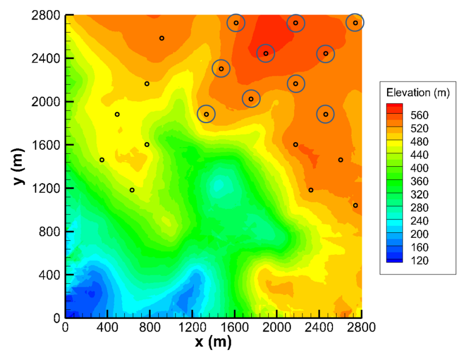

(b) Second iteration

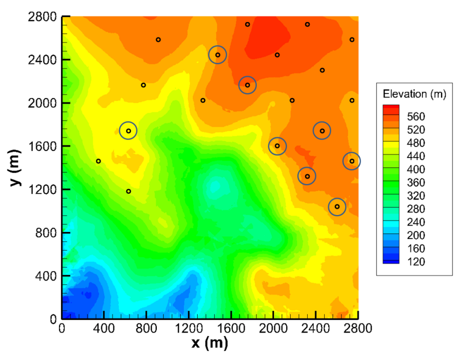

(c) Third iteration

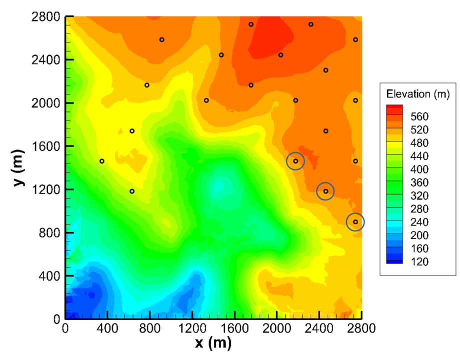

(d) Fourth iteration

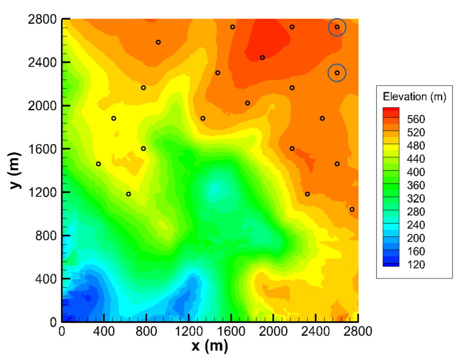

(e) Fifth iteration

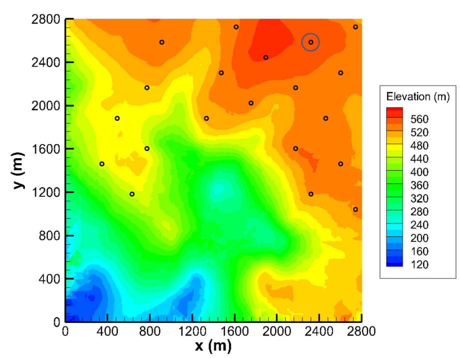

(f) Sixth iteration

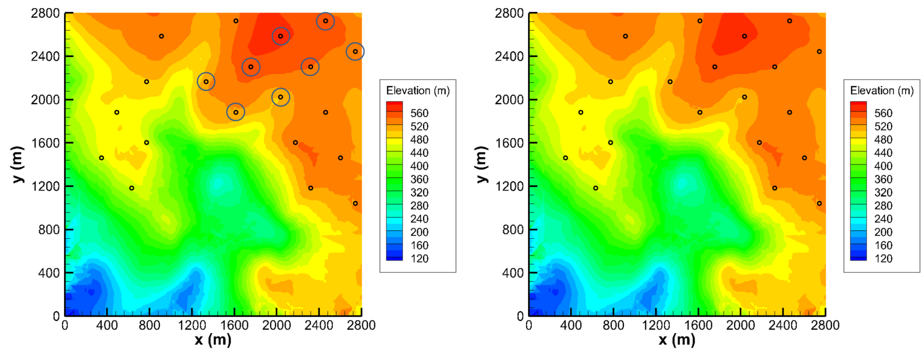

(g) Seventh iteration

(h) Eighth iteration

Figure 12: Optimal layout found at the end of each iteration with relaxation parameter, C, set to 0. The circles mark the turbines that were relocated in that iteration. Note that after 8 iterations, the algorithm did not identify additional turbine locations that would lead to improvements in the optimization objective.

5. Concluding Remarks

In this work, an algorithm that optimizes wind farm layouts on complex terrains was introduced. This algorithm combines CFD simulations with mathematical programming methods for layout optimization. To the best of the authors' knowledge, this is the first WFLO study that makes use of mathematical programming methods with CFD wake simulations. The proposed iterative approach identifies promising turbine locations to minimize the number of CFD simulations required in optimization while finding good layouts, even when the optimization relies on inaccurate wake models during the first iterations. The proposed approach starts with an approximate wake model that superimposes a flat terrain wake model on the topography, and this model is adaptively refined based on CFD simulations that are conducted only at promising turbine locations. This paper presents a better and more efficient optimization of wind turbine layouts on complex terrain, because of better modeling accuracy and the theoretical convergence bounds of MIP models.

In order to study the effects of initial wake approximation on solution quality

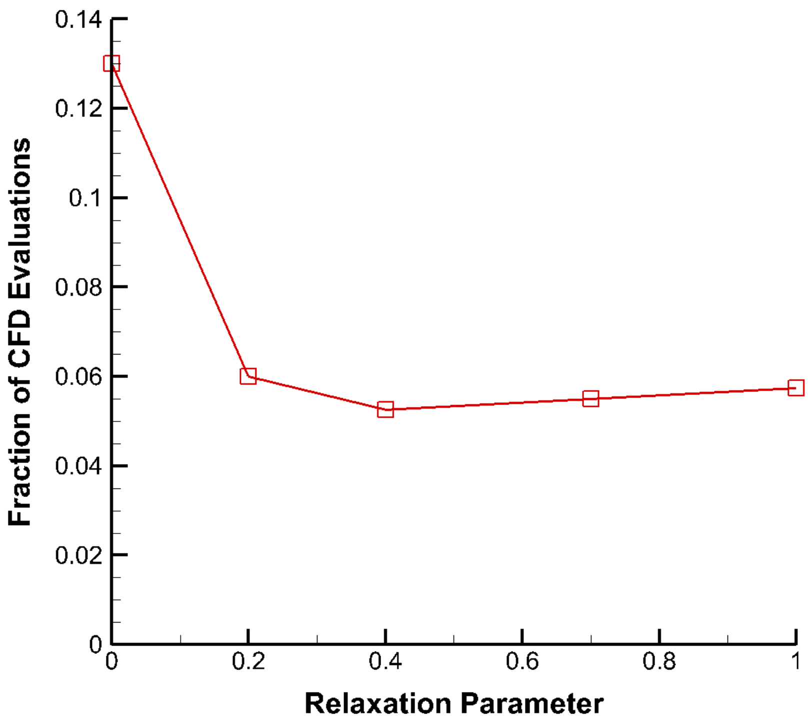

Figure 13: Effects of relaxation parameter on computational cost (fraction of maximum number of CFD evaluations).

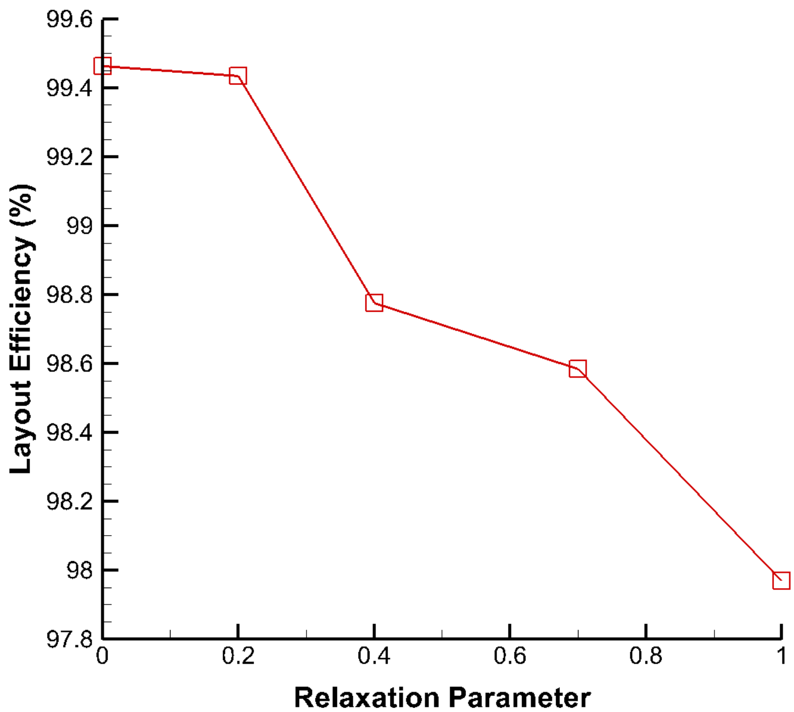

Figure 14: Effects of relaxation parameter on layout efficiency.

and computational cost, we introduced a relaxation parameter to control how the optimization space is explored. It was found that regardless of the parameter value, the difference in performance for best and worst layouts found is less than 1.5%, indicating that the algorithm is capable of finding good layouts even under poor initial wake approximations. Finding a suitable value for the relaxation parameter will depend on the balance between computational cost and solution quality as low values of the relaxation parameter may improve solution quality at the expense of computational cost while the the reverse may hold true for high values.

Further work in developing the proposed novel approach for WFLO combining CFD simulations of wake behavior with mathematical programming is needed to study the scalability of the algorithm to larger problem instances, i.e., to wind farms with more potential turbine locations. The implications of this work are that CFD can be a valuable tool in WFLO problems and that good potential turbine locations can be identified in advance to significantly reduce the number of expensive simulations.

6. Acknowledgment

This work was supported by the Natural Sciences and Engineering Research Council of Canada (NSERC) and Hatch Ltd., under grant CRDPJ 437325-12. The authors gratefully acknowledges financial support provided by the NSERC Canada Graduate Scholarship and Hatch Graduate Scholarship for Sustainable Energy Research.

References

[1] R. J. Barthelmie, K. Hansen, S. T. Frandsen, O. Rathmann, J. G. Schepers, W. Schlez, J. Phillips, K. Rados, A. Zervos, E. S. Politis, P. K. Chaviaropoulos, Modelling and measuring flow and wind turbine wakes in large wind farms offshore, Wind Energy 12 (5) (2009) 431–444.

[2] P. Y. Zhang, Topics in wind farm layout optimization: Analytical wake models, noise propagation, and energy production, Master's thesis, University of Toronto (2013).

[3] S. Turner, D. Romero, P. Zhang, C. Amon, T. Chan, A new mathematical programming approach to optimize wind farm layouts, Renewable Energy 63 (2014) 674–680.

[4] G. Mosetti, C. Poloni, B. Diviacco, Optimization of wind turbine positioning in large windfarms by means of a genetic algorithm, Journal of Wind Engineering and Industrial Aerodynamics 51 (1) (1994) 105–116.

[5] S. Grady, M. Hussaini, M. Abdullah, Placement of wind turbines using genetic algorithms, Renewable Energy 30 (2) (2005) 259–270.

[6] J. Park, K. H. Law, Layout optimization for maximizing wind farm power production using sequential convex programming, Applied Energy 151 (2015) 320 – 334.

[7] X. Gao, H. Yang, L. Lu, Study on offshore wind power potential and wind farm optimization in hong kong, Applied Energy 130 (2014) 519 – 531.

[8] J. Feng, W. Z. Shen, Wind farm layout optimization in complex terrain: A preliminary study on a gaussian hill, in: Journal of Physics: Conference Series, Vol. 524, IOP Publishing, 2014, p. 012146.

[9] M. Song, K. Chen, Z. He, X. Zhang, Wake flow model of wind turbine using particle simulation, Renewable energy 41 (2012) 185–190.

[10] M. Song, K. Chen, Z. He, X. Zhang, Bionic optimization for micro-siting of wind farm on complex terrain, Renewable Energy 50 (2013) 551–557.

[11] M. Song, K. Chen, Z. He, X. Zhang, Optimization of wind farm micro-siting for complex terrain using greedy algorithm, Energy 67 (2014) 454–459.

[12] M. Song, K. Chen, X. Zhang, J. Wang, The lazy greedy algorithm for power optimization of wind turbine positioning on complex terrain, Energy 80 (2015) 567 – 574.

[13] A. E. Kasmi, C. Masson, An extended model for turbulent flow through horizontal-axis wind turbines, Journal of Wind Engineering and Industrial Aerodynamics 96 (1) (2008) 103 – 122.

[14] J. Prospathopoulos, E. Politis, K. Rados, P. Chaviaropoulos, Evaluation of the effects of turbulence model enhancements on wind turbine wake predictions, Wind Energy 14 (2) (2011) 285–300.

[15] Y.-T. Wu, F. Porté-Agel, Atmospheric turbulence effects on wind-turbine wakes: An les study, Energies 5 (12) (2012) 5340–5362.

[16] A. Makridis, J. Chick, Validation of a cfd model of wind turbine wakes with terrain effects, Journal of Wind Engineering and Industrial Aerodynamics 123 (2013) 12–29.

[17] J. Schmidt, B. Stoevesandt, Modelling complex terrain effects for wind farm layout optimization, in: Journal of Physics: Conference Series, Vol. 524, IOP Publishing, 2014, p. 012136.

[18] J. Schmidt, B. Stoevesandt, Wind farm layout optimization in complex terrain with cfd wakes.

[19] R. Barthelmie, S. Pryor, An overview of data for wake model evaluation in the virtual wakes laboratory, Applied Energy 104 (2013) 834 – 844.

[20] P. Y. Zhang, D. A. Romero, J. C. Beck, C. H. Amon, Solving wind farm layout optimization with mixed integer programs and constraint programs, EURO Journal on Computational Optimization 2 (3) (2014) 195–219.

[21] J. Y. Kuo, D. A. Romero, C. H. Amon, A novel wake interaction model for wind farm layout optimization, in: ASME 2014 International Mechanical Engineering Congress and Exposition, American Society of Mechanical Engineers, 2014.

[22] J. Y. Kuo, D. A. Romero, C. H. Amon, A mechanistic semi-empirical wake interaction model for wind farm layout optimization, Energy 93 (2015) 2157–2165.

[23] A. Schrijver, Theory of linear and integer programming, John Wiley & Sons, 1998.

[24] P. Fagerfjäll, Optimizing wind farm layout–more bang for the buck using mixed integer linear programming, Master's thesis, Chalmers University of Technology and Gothenburg University (2010).

[25] S. Donovan, An improved mixed integer programming model for wind farm layout optimisation, in: Proceedings of the 41th Annual Conference of the Operations Research Society. Wellington, New Zealand, 2006.

[26] A. Mittal, Optimization of the layout of large wind farms using a genetic algorithm, Ph.D. thesis, Case Western Reserve University (2010).

[27] A. Kusiak, Z. Song, Design of wind farm layout for maximum wind energy capture, Renewable Energy 35 (3) (2010) 685–694.

[28] B. L. Du Pont, J. Cagan, An extended pattern search approach to wind farm layout optimization, Journal of Mechanical Design 134 (2012) 081002.

[29] S. Chowdhury, J. Zhang, A. Messac, L. Castillo, Unrestricted wind farm layout optimization (uwflo): Investigating key factors influencing the maximum power generation, Renewable Energy 38 (1) (2012) 16–30.

[30] J. Serrano Gonzalez, M. Burgos Payan, J. Riquelme Santos, Wind farm optimal design including risk, in: Modern Electric Power Systems (MEPS), 2010 Proceedings of the International Symposium, IEEE, pp. 1–6.

[31] W. Kwong, P. Zhang, D. Romero, J. Moran, M. Morgenroth, C. Amon, Wind farm layout optimization considering energy generation and noise propagation, in: Proceedings of the ASME 2012 International Des Engineering Technology Conference & Computing and Information in Engineering Conference. Chicago, IL, USA., 2012, pp. 1–10.

[32] L. Chen, E. MacDonald, Considering landowner participation in wind farm layout optimization, Journal of Mechanical Design 134 (2012) 084506.

[33] L. Chen, E. MacDonald, A system-level cost-of-energy wind farm layout optimization with landowner modeling, Energy Conversion and Management 77 (2014) 484–494.

[34] J. Feng, W. Z. Shen, Solving the wind farm layout optimization problem using random search algorithm, Renewable Energy 78 (2015) 182–192.

[35] Y. Chen, H. Li, K. Jin, Q. Song, Wind farm layout optimization using genetic algorithm with different hub height wind turbines, Energy Conversion and Management 70 (2013) 56 – 65.

[36] Y. Chen, H. Li, B. He, P. Wang, K. Jin, Multi-objective genetic algorithm based innovative wind farm layout optimization method, Energy Conversion and Management 105 (2015) 1318–1327.

[37] B. Saavedra-Moreno, S. Salcedo-Sanz, A. Paniagua-Tineo, L. Prieto, A. Portilla-Figueras, Seeding evolutionary algorithms with heuristics for optimal wind turbines positioning in wind farms, Renewable Energy 36 (11) (2011) 2838–2844.

[38] S. Chowdhury, J. Zhang, A. Messac, L. Castillo, Characterizing the influence of land configuration on the optimal wind farm performance, in: ASME 2011 International Design Engineering Technical Conferences & Computers and Information in Engineering Conference (IDETC/CIE 2011), No. DETC2011-48731, ASME. Washington, DC, USA, 2011.

[39] A. Chehouri, R. Younes, A. Ilinca, J. Perron, Review of performance optimization techniques applied to wind turbines, Applied Energy 142 (2015) 361 – 388.

[40] B. P. Rašuo, A. Č. Bengin, Optimization of wind farm layout, FME Transactions 38 (3) (2010) 107–114.

[41] B. Pérez, R. Mínguez, R. Guanche, Offshore wind farm layout optimization using mathematical programming techniques, Renewable Energy 53 (2013) 389–399.

[42] M. Wagner, J. Day, F. Neumann, A fast and effective local search algorithm for optimizing the placement of wind turbines, Renewable Energy 51 (2013) 64–70.

[43] J. Cleve, M. Greiner, P. Enevoldsen, B. Birkemose, L. Jensen, Model-based analysis of wake-flow data in the nysted offshore wind farm, Wind Energy 12 (2) (2009) 125–135.

[44] J.-O. Mo, A. Choudhry, M. Arjomandi, Y.-H. Lee, Large eddy simulation of the wind turbine wake characteristics in the numerical wind tunnel model, Journal of Wind Engineering and Industrial Aerodynamics 112 (2013) 11–24.

[45] Y.-T. Wu, F. Porté-Agel, Large-eddy simulation of wind-turbine wakes: evaluation of turbine parametrisations, Boundary-layer meteorology 138 (3) (2011) 345–366.

[46] H. Zhong, P. Du, F. Tang, L. Wang, Lagrangian dynamic large-eddy simulation of wind turbine near wakes combined with an actuator line method, Applied Energy 144 (2015) 224 – 233.

[47] E. S. Politis, J. Prospathopoulos, D. Cabezon, K. S. Hansen, P. Chaviaropoulos, R. J. Barthelmie, Modeling wake effects in large wind farms in complex terrain: the problem, the methods and the issues, Wind Energy 15 (1) (2012) 161–182.

[48] R. Mikkelsen, Actuator disc methods applied to wind turbines, Ph.D. thesis, Technical University of Denmark (2003).

[49] F. Castellani, A. Vignaroli, An application of the actuator disc model for wind turbine wakes calculations, Applied Energy 101 (2013) 432 – 440, sustainable Development of Energy, Water and Environment Systems.

[50] N. Troldborg, J. N. Sørensen, R. Mikkelsen, Actuator line simulation of wake of wind turbine operating in turbulent inflow, in: Journal of Physics: Conference Series, Vol. 75, IOP Publishing, 2007, p. 012063.

[51] L. A. Martınez, S. Leonardi, M. J. Churchfield, P. J. Moriarty, A comparison of actuator disk and actuator line wind turbine models and best practices for their use, AIAA Paper (2012-0900).

[52] F. Porté-Agel, H. Lu, Y.-T. Wu, Interaction between large wind farms and the atmospheric boundary layer, Procedia IUTAM 10 (2014) 307–318.

[53] P.-E. M. Réthoré, N. N. Sørensen, F. Zahle, Validation of an actuator disc model, in: 2010 European Wind Energy Conference and Exhibition, 2010.

[54] P.-E. Réthoré, P. Laan, N. Troldborg, F. Zahle, N. N. Sørensen, Verification and validation of an actuator disc model, Wind Energy 17 (6) (2014) 919–937.

[55] A. El Kasmi, C. Masson, An extended k–ε model for turbulent flow through horizontal-axis wind turbines, Journal of Wind Engineering and Industrial Aerodynamics 96 (1) (2008) 103–122.

[56] GE Energy, 1.5MW Wind Turbine, Tech. rep., General Electric (2009).

[57] Environment Canada, Canadian Wind Energy Atlas (2011).
URL `http://www.windatlas.ca/en/index.php`

[58] B. Blocken, T. Stathopoulos, J. Carmeliet, Cfd simulation of the atmospheric boundary layer: wall function problems, Atmospheric environment 41 (2) (2007) 238–252.

[59] J. Prospathopoulos, E. Politis, P. Chaviaropoulos, Modelling wind turbine wakes in complex terrain, Proceedings EWEC 2008, Brussels, Belgium.

[60] L. Davis, Genetic algorithms and simulated annealing.